AGILE: GIScience Series, 6, 41, 2025. https://doi.org/10.5194/agile-giss-6-41-2025
Proceedings of the 28th AGILE Conference on Geographic Information Science, 10–13 June 2025.
Eds.: Auriol Degbelo, Serena Coetzee, Carsten Keßler, Monika Sester, Sabine Timpf, Lars Bernard
This contribution underwent peer review based on a full paper submission.

Do green roofs and spatial resolution influence flood simulation output? – A case study in Malmö, Southern Sweden

Karolina Pantazatou [1], Andreas Persson [1], and Per-Ola Olsson [1], and Lars Harrie [1]

[1] Department of Physical Geography and Ecosystem Science, Lund University, Lund, Sweden.

Correspondence: Karolina Pantazatou (karolina.pantazatou@nateko.lu.se)

Abstract. Over recent years many urban areas have experienced severe floods caused by extreme precipitation events. To avoid the devastating socioeconomic and environmental consequences of such floods, countries have issued laws or recommendations on flood risk assessment in urban planning. However, these laws or recommendations seldom include detailed requirements on input data quality or explicit instructions regarding flood simulation settings, leaving much open to interpretation. To contribute to the solution of this issue, this study focuses on examining the influence of the spatial resolution of input data (e.g., elevation and land cover) on flood simulations for urban densification planning, implementing 100-year return period precipitation scenarios. It also explores the impact of green roofs on flood simulations implementing 10-year and 20-year return period precipitation scenarios within the same context. The results show that spatial resolution may affect simulation output since the areas' land-cover differs but also because of how edge cells are treated in flow simulations. Green roofs and the drainage from these relieve the ground from being flooded with 20-27% less water.

Submission Type. Analysis; Case study; Model

BoK Concepts. GI and Society; Geospatial Data; Geocomputation

Keywords. flood simulations, TFM-DYN, green roofs, CityGML, sustainable urban planning

1 Introduction

Extreme precipitation events have increased in frequency and intensity over the past two decades as a direct result of climate change (Lehmann et al., 2015; Fowler et al., 2021; Robinson et al., 2021). Cities are particularly vulnerable to floods, since they are often characterized by densely built-up areas with few open spaces reserved for parks and recreational areas (Kabisch & Haase, 2012; Karteris et al., 2016). The problem is getting even worse as cities are being densified (Hemmati et al., 2020; UN, 2018). To cope with this situation urban planners, create flood resilience plans which offer a framework for addressing both extreme rainfall flooding and the uneven effects of such events. One input to these plans are flood simulations.

Though many countries have introduced laws or recommendations making flood simulations compulsory in urban planning, these seldomly include detailed requirements on input data quality and simulation settings (Directive 2007/60/EC; Länsstyrelserna, 2018). This input could come from e.g. 3D city models. To assist in bridging the gap, this study examines the influence of:

- the spatial resolution of input data (e.g., elevation and land cover) on flood simulations in real-world urban densification scenarios
- including green roof information in flood simulations.

The study is linked to the formation of a Swedish national profile (3CIM) for a semantic 3D city model, implemented as a CityGML ADE (Uggla et al., 2023). The ambition is that 3CIM will support all simulations required in the urban planning process.

2 Background

There are many flood simulation tools available, which can ultimately be divided into two categories: *physically-*

based and *elevation-based* hydrological models. Physically-based models try to describe the physical processes in detail and are dynamic in the sense that they produce results over time. However, they are often tedious to set up with many parameters. Elevation-based models can in the simplest form estimate the water movement with elevation data as the sole input. In this case, the result is a static map of how flow accumulates downhill in a landscape. Some elevation-based models have been developed to also include some physical processes and the possibility of dynamic simulations. The TFM-DYN is such a model, based on *Digital Terrain Model* (DTM), *Digital Surface Model* (DSM) and *land cover* (LC) data. With the addition of surface roughness and infiltration capacity, TFM-DYN estimates the flow in raster elevation models with a given input of precipitation (Nilsson et al., 2021). With a better flow distribution algorithm than what is generally provided in GIS software and in many hydrological models, it distributes water in a realistic way with a proportional distribution to lower parts of the landscape (Pilesjö and Hasan, 2014). Velocity is altered according to the *Manning* formula (Tuozzolo et al., 2019) and an infiltration deduction in permeable surfaces can be set. With a higher frequency of extreme weather events such as cloudbursts, simulations for climate adaptation need to be carried out over both large areas and local parts of cities. With shorter setup and simulation time a model like TFM-DYN can provide the possibility of exploring several scenarios (Persson et al., 2024). Different types of precipitation events can be simulated on a landscape that itself can be altered. Alterations may be considered for the DTM, DSM and LC data, e.g. water barriers and green roofs.

In the simulations, the DTM provides information on land surface topography while the DSM provides elevation information for ground surfaces and above-ground structures (e.g., buildings). The land surface topography information included in a DSM is essential for the prediction of surface flows including *flow depth* (i.e., water depth on the ground), *water-surface slope* (i.e., slope gradient between cells calculated based on the sum of ground and water levels for each cell), *mean flow velocity* (i.e., velocity of water moving from one cell to another, during a specific time step), and *flow discharge* (i.e., volume of water moving from one cell to another during a specific time step) (Casas et al., 2006; Azizian & Brocca, 2019). For a more detailed description of the aforementioned terms please refer to Persson et al. (2024). The simulations require detailed DTM and DSM data (Pizzileo et al., 2024) which commonly are derived from aerial laser scanning data.

LC-data contains information on the physical material of a ground surface (e.g., grass) and should not be confused with *land use* (LU) which describes how the ground surface is utilized (e.g., park, sports facility – football court). Since every material has different physical properties, LC information is crucial for determining the permeability of ground surfaces (infiltration) and friction affecting surface flows in flood simulations (Brody et al., 2013; Persson et al., 2024). Though some materials might have a fixed infiltration capacity (e.g., *asphalt*), this is not the case for materials like *grass* or *bare soil* whose water absorption capacity is influenced by climate and depends on the state they are in (dry, healthy/moist, wet).

LC information is available in different formats (raster, vector) and quality, but creating it is a complex and time-consuming task, often necessitating the processing of multiple datasets from various sources (Ahlkrona et al., 2018). Typical examples of pan-European open access LC datasets are CORINE and Urban Atlas. The former has a spatial resolution of 100m and covers Europe, while the latter has a spatial resolution of 10m but is only available for a subset of cities; both have a very low temporal updating frequency (6 years) (Büttner, 2014; European Environmental Agency, 2021). Additionally, several countries offer open-access national LC datasets, usually derived from satellite remote sensing data with higher spatial resolution than CORINE (Ahlkrona et al., 2018; Büttner, 2014), while municipalities gather detailed LU data for urban planning, using aerial images or high-resolution satellite images (Belgiu et al., 2013), LiDAR data (Yan et al., 2014), and sometimes terrestrial observations.

Flood simulations are complex, computationally intensive, and can take long time to execute. One of the most time-consuming tasks when executing flood simulations is to find, access, and prepare input data (Gichamo et al., 2020). One attempt to reduce the time required to find and download flood simulation input datasets is to make *semantic 3D city models* support those simulations. Semantic 3D city models are digital 3D representations of urban environments with the capacity to store semantic information for every geometric object (e.g., building address, roof material, etc.) (Gröger et al., 2012). The Open Geospatial Consortium (OGC) has introduced the CityGML standard for such models (Gröger et al., 2012; Kolbe et al., 2021). CityGML encompasses various themes (e.g., *Building*, *Transportation*, *Vegetation*, *LandUse*, *Relief*, etc.), facilitating the storage of DSM, DTM, LC data and other data (e.g., buildings) used as input to flood simulations. Moreover, CityGML can be extended to accommodate the storage of additional information required by specific applications with *Application Domain Extensions* (ADE) (Gröger et al., 2012; Biljecki et al., 2018). A flood ADE was proposed by Shen et al. (2020) and a HydroADE by Schulte & Coors (2008).

Green roofs have been considered suitable to stall the flow of pluvial rain (Chan et al., 2022). Several countries have imposed restrictions regarding the inclination of green roofs. In Sweden, the roof inclination threshold is set to 30 degrees. Though the use of green roofs in certain countries has been extensive (Köhler, 2006; Graceson et al., 2013), detailed official registers of which roofs are green are not always available. This information could of course be obtained by combining open-access building footprint data from national mapping agencies with vegetation indices like NDVI from remote sensing, but doing so would still require additional processing time and effort. Information on which roofs or which parts of a roof are green can be stored as an attribute in the *Building* theme of CityGML using *ADEOfRoofSurface*, which acts as a hook to define properties within an ADE that are to be added to a *RoofSurface* (Kolbe et al., 2021).

The European Union (EU) has issued a directive for Floods (Directive 2007/60/EC) requiring all EU countries to: (1) evaluate areas with a high risk for severe flooding, (2) map the extent of potential flooding and identify the assets and people at risk in these areas, and (3) implement appropriate and coordinated actions to minimize flood risks. No explicit instructions are provided regarding specific simulation settings or input data requirements.

In Sweden, flood risk assessments required for urban planning are typically conducted early in the planning process. The municipal urban planning office is responsible for managing land and water use, as outlined in legally binding documents (e.g., detailed development plans), but the County Administrative Board (CAB, in Swedish: *Länsstyrelsen*) can veto these plans. Since 2018, municipalities must include flood risk assessments in their plans, and the CAB provides guidance on how to conduct these assessments. The CABs have issued some recommendations on flood analysis, but these are rarely converted into strict guidelines for input data (Länsstyrelserna, 2018). The only specific recommendations regarding input data and flood simulation settings are the following:

- DTM/DSM of at least 2×2m spatial resolution should be used in flood risk assessments conducted over detailed development plans.
- Flood risk assessments for detailed development plans should be conducted executing simulations implementing 100-year return period precipitation events.
- The climate factor should be at least 1.2. (Explanation: To transfer the climate change effects and possible future changes, the estimated rainfall value is multiplied by climate factor (Alipour et al., 2023). Climate factors are estimated based on return period, rainfall duration, geographical location, reference period, scenario period and climate models (global/regional) (Hanssen-Bauer et al., 2009).

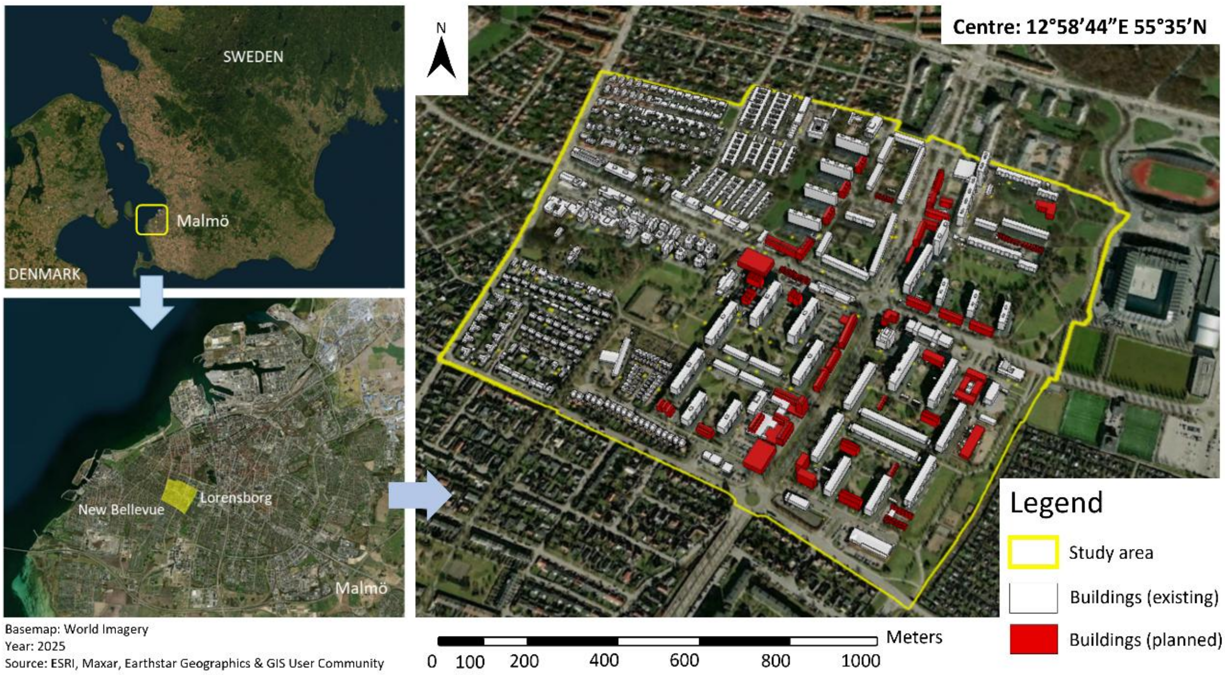

Figure 1. Study area – New Bellevue and Lorensborg neighbourhoods in Malmö, southern Sweden.

3 Data and methods

3.1 Study area

The study area, located in the new Bellevue and Lorensborg neighborhoods of Malmö, Sweden, spans approximately 945,000 m² (Fig. 1). It was selected due to its recent designation as suitable for urban densification and because it is close to an area that quite recently experienced a severe flood (Hernberg et al., 2015). The study area is primarily residential, with a mix of villas and 3-6 story buildings. The land cover is diverse, featuring both vegetated spaces and built-up surfaces near the city center. It is a relatively flat region with elevation ranging 7-18m above sea level (Fig. A.1). The study area is dominated by buildings with gabled roofs, where tall buildings have roofs with very low inclinations while villas and lower multistory buildings have higher roof inclinations.

3.2 Data and tools

Input data to flood simulations include 3D building information, a DTM and LC data (Table 1).

Table 1. Description of flood simulation input datasets.

Dataset	Format	CRS/ VCS	Source	Access	Spatial resolution/ LOD
3D buildings	OBJ	EPSG: 3008 VCS: RH2000	Malmö municipality (MM)	Accessible with payment	CityGML LOD2
3CIM Buildings (planned/ existing)	CityGML	EPSG: 3008 VCS: RH2000	MM + Uggla et al. (2023)	Open access	CityGML LOD2
LC	ESRI shapefile (vector)	EPSG: 3008	MM + Pantazatou et al. (2025)	Open access	Spatial accuracy on dm level
DTM	GeoTIFF	EPSG: 3008 VCS: RH2000	Malmö municipality	Accessible with payment	1m spatial resolution

For this study, we used a LiDAR-derived DTM (spatial resolution: 1m) from Malmö municipality. 3D building information for planned as well as existing buildings was derived from the 3CIM test data (Uggla et al., 2023) in Malmö where the areas overlap; for the remaining of the study area the buildings were obtained from Malmö municipality's 3D city model. Elevation in original DTM and 3D building datasets is expressed as distance from the geoid. LC data was digitised manually using Malmö municipality's basemap (year: 2018) overlayed over an orthophoto (source: Malmö municipality, 0.08m spatial resolution, year: 2018). The LC thematic classes follow the latest proposed version of the Swedish National Specifications for LC (NS-LC). Table A.1 presents the LC classes in conjunction with their corresponding infiltration value. More details regarding the construction of the LC-dataset are provided in Pantazatou et al. (2025).

3.3 Methods/scenarios

3.3.1 Pre-processing of input data

To follow the Swedish regulations for green roofs (maximum inclination ≤ 30°), all roofs for planned buildings were changed to an inclination ≤ 30°, if their initial roof inclination was higher. 3D buildings were converted from CityGML to Multipatch shapefiles and rasterized. DTM areas covered by buildings were masked out and replaced by the elevation values of the rasterized buildings to produce the DSM (Fig. A.2).

The initial LC vector dataset was rasterized. The DSM was cut to the extent of the rasterized LC dataset. The rasterized 3D building information included roof overhang, but the rasterized LC did not. To ensure that cells representing building area in the DSM also represented building area in the LC, we implemented the steps described in Fig. A.3-A.4. The processes in Fig. A.2-A.4 were repeated for all spatial resolutions examined in the study.

3.3.2 Simulation scenarios

To test the influence of spatial resolution on flood simulations, we executed simulations for the scenarios in Table 2. These scenarios represent a set of tests that municipalities are required to perform when planning new constructions. They cover an extreme case of a cloudburst with an intensity of a 100 year's return period rain event. They also cover an event of a 10 years return period which is the historical norm for what the urban storm sewage system should be able to handle, and which is what it is dimensioned for in areas subject to densification. To test an event that in a closer future will have a higher frequency, like the present 10-years return period event, we also test a 20-years return period event for scenarios considering green roofs. The simulations were run for rasters with resolutions of 4×4, 1×1 and 0.5×0.5 meters.

Table 2. Simulations of return period events, the resolutions simulated and the building scenarios before densification (BD) and after densification (AD).

Raster resolutions (m)	4x4			1x1			0.5x0.5		
Event return period	100	20	10	100	20	10	100	20	10
BD: No green roofs	x			x		x	x		x
BD: Green roofs						x			x
AD: No green roofs	x	x		x	x	x	x	x	x
AD: Green roofs		x			x	x		x	x

3.3.3 Precipitation scenarios

The Swedish Meteorological and Hydrological Institute (SMHI) has calculated, based on regional observations of cloudbursts, the return periods and intensities of extreme precipitation (Olsson et al., 2017). This data is the base of the three precipitation scenarios used in this study. The three precipitation scenarios are presented in Table 2. All scenarios start with a 30minute, 2-years return period heavy rain event. After that a cloudburst event takes place for another 30 minutes. These events are a 100-years return period event, a 10-years return period event and a 20-year return period event. After the heavy rain events, the simulations continue for 10 more minutes for water to flow further downstream. The following tables (Tables 3.a – 3.c) summarize the cloudburst scenarios related to every precipitation scenario (100-year, 20-year, 10-year) presented in Table 2.

Table 3.a 100 years return period cloudburst scenario

30 min 2-yr return period rain event	13.1mm
30 min 100-yr return period rain event	38.8 mm
10 min without precipitation	0 mm

Table 3.b 10 years return period cloudburst scenario

30 min 2-yr return period rain event	13.1 mm
30 min 10-yr return period rain event	20.5 mm
10 min without precipitation	0 mm

Table 3.c 20 years return period cloudburst scenario

30 min 2-yr return period rain event	13.1 mm
30 min 10-yr return period rain event	24.8 mm
10 min without precipitation	0 mm

4 Results & Discussion

This section includes the flood simulation results per scenario along with some LC-related supporting information to assist the assessment of the flood situation output.

The total area covered by green roofs is 3165 m^2 before the urban densification, and approximately 34360 m^2 after the densification. Planned buildings correspond to a total area of 31195 m^2, while existing buildings cover an area of 154980 m^2. Green roofs cover 2% of the total building roof area before the densification and 18.5% of the total building roof area after the densification. Fig. 5 displays the distribution of LC classes covering areas corresponding to planned buildings.

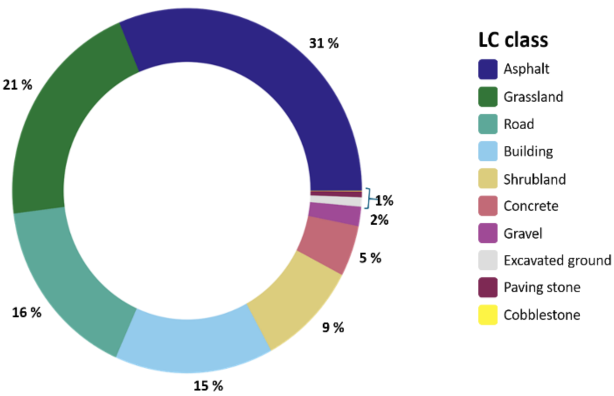

Figure 5. Breakdown of LC classes replaced by planned buildings.

Table 4 describes the land surface as impermeable if its capacity is 0-2 mm/h (see Table A.1). It should be noted that the differences in permeable/impermeable land when comparing scenarios considering green roofs to those that do not, are quite small. Before the urban densification is carried out the differences between permeable and impermeable land range between 0.3-04% for scenarios that consider green roofs compared to those that do not. After the densification, the corresponding differences range between 3.57-3.65%.

Table 4. Percentage area of permeable/impermeable land per simulation scenario.

Densification	Green roofs	Spatial resolution	Permeable areas (%)	Impermeable areas (%)
BD	No	4m	48.2%	51.8%
BD	No	1m	48.3%	51.7%
BD	No	0.5m	48.3%	51.7%
BD	Yes	1m	48.6%	51.4%
BD	Yes	0.5m	48.6%	51.4%
AD	No	4m	47.2%	52.8%
AD	No	1m	47.2%	52.8%
AD	No	0.5m	47.3%	52.7%
AD	Yes	1m	50.85%	49.15%
AD	Yes	0.5m	50.87%	49.13%

The dynamic simulations are performed with a sub-second time step and generate, among other (see Persson et al., 2024), results for water depths per raster cell, total amount of water moved in the area studied, infiltrated water per cell and total water infiltrated in the whole area studied. They also generate a raster image at stages defined by the user. In this study we have generated images every 5 minutes of the event simulated. Fig. 6-7 present the water depth situation at 30 and 60 minutes for the simulation before densification, with no green roofs present, in the 4 m raster, with a 100-year return period

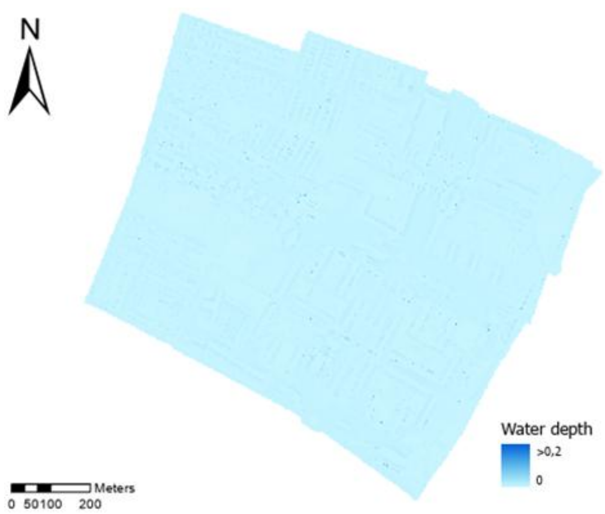

Figure 6. Water depth after 30 min event simulation time in the 100-year return period scenario, BD without green roofs.

cloudburst. The major changes are seen in the lowest areas of the landscape and the largest parts of the area have a water level of 1-4 cm water depth both at 30 and 60 minutes. The same patterns are observed in all simulation outputs of the study.

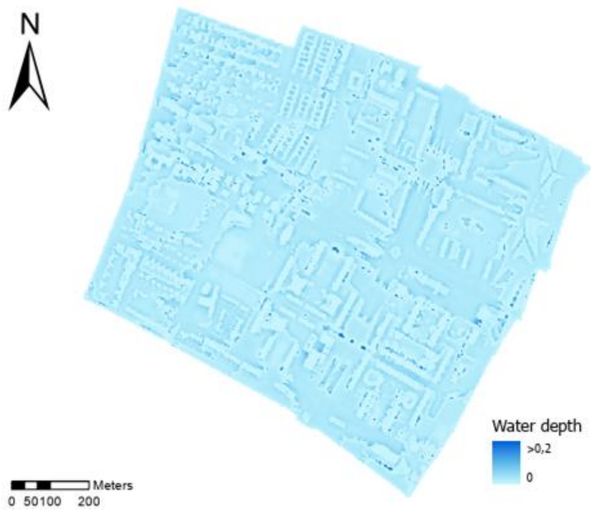

Figure 7. Water depth after 60 min event simulation time in the 100-year return period scenario, BD without green roofs.

Another approach is to analyse the data for total water volumes in the dataset at the different timestamps 30, 60 and 70 minutes. This shows how both the spatial resolution and the green roofs affect the results. In Fig. 8, the effect of a coarse resolution is most obvious. The 4m resolution generate a lower volume than the 0.5m and 1m resolution. Compared to a 1m resolution, the 0.5 generate approximately 1% more water at all time stages. The 4m resolution on the other hand simulate 3-4.5% less water at the timestamps presented. This equals at the latter stages 775-875m^3.

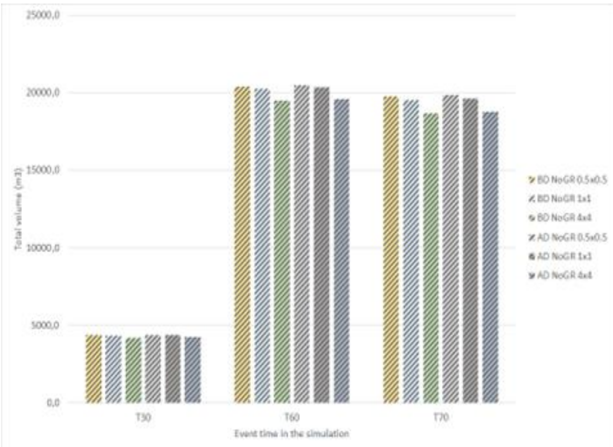

Figure 8. Total volume of water in simulation of 100-year return period cloudburst BD & AD, no green roofs.

The reason for this difference is not found in a difference of permeable areas (Table 4) but rather in the handling of the raster. Boundary cells are not subject to simulation since they lack neighbours in some directions and the total volumes of precipitation water in these cells are not included in the simulation. In a coarse resolution this effect gives a larger impact on the values than on a raster with a high resolution since the area excluded is smaller. For climate adaptation measures and dimensions of storm water systems this needs to be considered when simulations are used for decision support.

As seen in the data of infiltrated water the effect of spatial resolution is smaller. The difference of infiltration is less than 1% between the 4m and 1m resolution while the 0.5m resolution differ up to 1.2% in relation to the 1m resolution. The 1m resolution infiltrate the most water as seen in Fig. 9. The smaller differences may be due to the number of infiltrable cells are mostly interior in the study area. The delineation of the area was made along roads which are impermeable and then cause a smaller effect on the total infiltration.

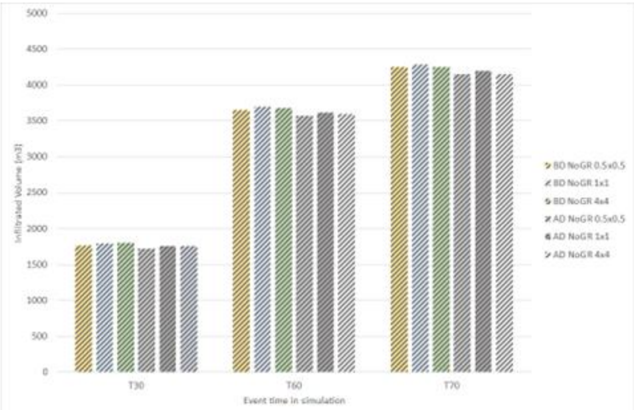

Figure 9. Total volume of water in simulation of 100-year return period cloudburst BD & AD, no green roofs.

The densification scenario with the 100-year return period event results in 0.4-0.9% more water in the system than before densification scenario.

In the 10-year return period cloudburst scenario the differences of total volumes of water in the raster at the studied timestamps between resolution 0.5m and 1m were approximately 1% for all scenarios except after densification with green roofs. In Fig. 10, it is possible to see that differences of total volumes of water ranged from 3-5% more water in the 0.5m resolution. This may be because planned buildings are situated on permeable areas, with higher infiltration capacity than the green roofs provide. A visual interpretation of the LC planned for densification show that this is the case. Even if the areas taken in consideration for densification are small, the classification of LC may be affected by the cell resolution, giving four cells per square meter in the 0.5m resolution compared to one in the 1m resolution.

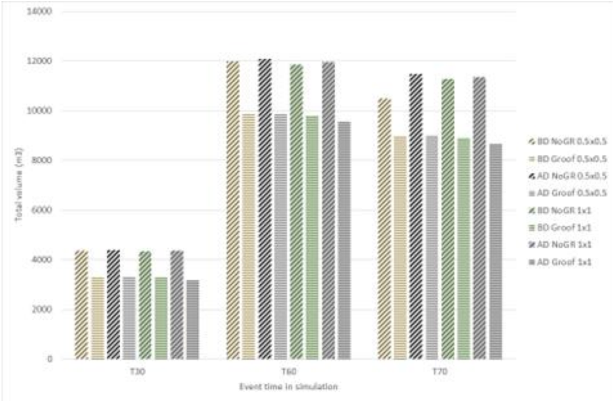

Figure 10. Total water volume in the 10-year return period cloudburst for 0.5m and 1m resolutions without (NoGR) and with (Groof) green roofs.

It is noteworthy that the amount of water in the system is mainly affected by the area of green roofs and the infiltration this provides, 20-27% less water compared to cases without green roofs. In this study the green roofs are given a high water-infiltrating capacity, like grass lawns. We motivate this with the assumption that excess water from these roofs will drain into the storm sewage system and will not end up in the volume on the ground. This is a generalisation made to test the system. In Fig. 11 it is seen that the amount of infiltrated water follows the pattern of water volume comparisons of green roof absence or presence.

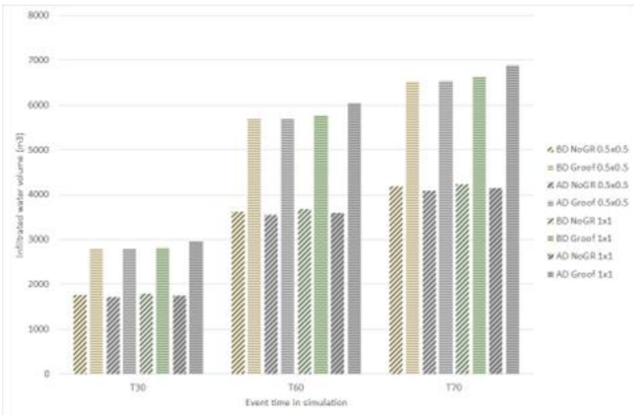

Figure 11. Total volumes of infiltrated water in the 10-year return period cloudburst for 0.5m and 1m resolutions without (NoGR) and with (Groof) green roofs.

Our study area is a typical example of northern European cities favouring green spaces (see Table 3) (Bille et al., 2023). If including information on green roofs is important for areas with almost 50% permeable surfaces (see Table 3), then this is even more important for urban areas with less permeable surfaces (or green areas) like the south of Europe (Bille et al., 2023) or in developing countries where quickly developing urban areas do not necessarily follow an urban plan and where spatial expansion occurs in the dense, informal settlements often termed “slums” that are typically lacking in infrastructure (Jha et al., 2012).

It should be noted that including green roof information in LC datasets is important not only from a flood simulation point of view. Also, other types of simulations (e.g., noise, daylight, etc.) that are required in the urban planning process as well as analyses performed to obtain a more sustainable urban environment (e.g., urban heat island) benefit from the inclusion of green roof information. For instance, green roofs should be considered in noise simulations, since they reflect/absorb noise differently than a concrete roof (Yang et al., 2011). From a daylight simulation perspective, including green roofs is important as vegetation reflects the incoming sunlight differently than a brick roof (Huang et al., 2023) and building materials have proved to have a significant effect on daylight reflectance in densely built-up urban areas (Pantazatou et al., 2023). In urban heat island studies, green surfaces (incl. green roofs) contribute to cooling the built-up environment (Razzaghmanesh et al., 2015). Finally, studies on urban biodiversity should include information about green roofs, as these vegetated surfaces enhance biodiversity by reducing the extent of densely built-up areas, providing suitable habitats for urban fauna, and supporting pollinators within city environments (Williams et al., 2014).

5 Conclusion

Given the complexity of implementing collaborative governance to effectively prepare for and mitigate the consequences of rare floods in urban regions (Hutter, 2015), providing explicit instructions regarding settings for urban flood simulation and their corresponding input data is important. Therefore, we propose the following:

- Use DSM of higher spatial resolution (<4m), since spatial resolution does affect flood simulation output to a large extent depending on the method. The influence of the spatial resolution of flood simulation input data becomes even more obvious when a high-accuracy routing model—designed for high-resolution data—is applied using coarse-resolution data, as this may cause edge effects that impact the simulation.
- Considering green roof information in flood simulations is advisable because it may affect the drainage and the water volumes that reach, or do not reach, the ground. Therefore, roof material information should be included in the semantic 3D city model (3CIM) and represented in one of the levels for the LC sub-class *Built-up surfaces; Building surfaces* or (alternatively) the sub-class *Built-up surfaces; Other built-up surfaces* in NS-LC.

Declaration of Generative AI in writing

The authors declare that they have not used Generative AI tools in the preparation of this manuscript. All intellectual and creative work, including the analysis and interpretation of data, is original and has been conducted by the authors without AI assistance.

Acknowledgements

We would like to thank Malmö municipality for providing the 3D city model used in our study. We would also like to express our gratitude to the Swedish Mapping, Cadastral, and Land Registration Authority (Lantmäteriet) for the constructive discussions and for kindly allowing us to use the current suggestion for NS-LC classifications.

Funding information

This work was supported by the Formas (Swedish Research Council for Sustainable Development) project *Facilitating energy and noise simulations in the planning of urban densification* [grant numbers 2020-01460].

Data and software availability

The research data for 3D buildings from 3CIM are available and accessible via the following link: https://www.smartbuilt.se/projekt/informationsinfrastruktur/3cim/

The research data for 3D buildings and DTM were accessed using the services at Malmö municipality (using a departmental subscription for costs). The compiled datasets cannot be redistributed due to licensing restrictions.

The research data for LC will become available in GitHub and is described in the following DOI: https://doi.org/10.1515/noise-2025-0016

Licensed commercial software: ESRI ArcGIS Pro 2.8.8, Safe's FME 2024.0.1 (ETL)

Flood simulation software: PluvioFlow AB's cloud-based realisation of TFM-DYN. www.pluvioflow.com

Hardware (simulation input data pre-processing): OS: Windows 11 Home, Processor: Intel(R) Core (TM) i7-10750H CPU @ 2.60GHz, RAM 16,0 GB (15,8 GB usable), System type: 64-bit operating system, x64-based processor.

Hardware (flood simulations): The simulation was performed on a Microsoft Azure F16s_v2 virtual machine instance with 16 vCPUs (Intel® Xeon® Platinum, 2.7-3.4 GHz), 32 GB RAM, and 256 GB temporary SSD storage.

References

Ahlkrona, E., Cristvall, C., Jönsson, C., Mattisson, A., & Olsson, B. (2018). National Land Cover layer for the counties of Scania, Blekinge, Kronoberg, Halland, Kalmar, Jönköpinge, Östergötland, Örebro: Product description. [*Nationella marktäckedata basskikt Skåne, Blekinge, Kronoberg, Halland, Kalmar, Jönköping, Östergötland, Örebro: Produktbeskrivning*]. In www.naturvardsverket.se. Swedish Environmental Protection Agency [*Naturvårdsverket*]. Retrieved February 6, 2025, from https://ext-dokument.lansstyrelsen.se/Ostergotland/Nationella%20Markt%C3%A4ckedata%20Produktbeskrivningar/NMD_Produktbeskrivning_Basskikt_regionA_v1.pdf

Alipour, S. M., Engeland, K., & Leal, J. (2023). Uncertainty analysis of 100-year flood maps under climate change scenarios. Journal of Hydrology, 628, 130502.https://doi.org/10.1016/j.jhydrol.2023.130502

Azizian, A., & Brocca, L. (2019). Determining the best remotely sensed DEM for flood inundation mapping in data sparse regions. International Journal of Remote Sensing, 41(5), 1884–1906. https://doi.org/10.1080/01431161.2019.1677968

Belgiu, M., Drăguţ, L., & Strobl, J. (2013). Quantitative evaluation of variations in rule-based classifications of land cover in urban neighbourhoods using WorldView-2 imagery. ISPRS Journal of Photogrammetry and Remote Sensing, 87, 205–215. https://doi.org/10.1016/j.isprsjprs.2013.11.007

Biljecki, F., Kumar, K., & Nagel, C. (2018). CityGML Application Domain Extension (ADE): overview of developments. Open Geospatial Data Software and Standards, 3(1). https://doi.org/10.1186/s40965-018-0055-6

Bille, R. A., Jensen, K. E., & Buitenwerf, R. (2023). Global patterns in urban green space are strongly linked to human development and population density. Urban Forestry & Urban Greening, 86, 127980. https://doi.org/10.1016/j.ufug.2023.127980

Brody, S., Blessing, R., Sebastian, A., & Bedient, P. (2013). Examining the impact of land use/land cover characteristics on flood losses. *Journal of Environmental Planning and Management*, *57*(8), 1252–1265. https://doi.org/10.1080/09640568.2013.802228

Büttner, G. (2014). *CORINE Land cover and land cover change products: Land use and land cover mapping in Europe: Practices & Trends*. Springer Netherlands.

Casas, A., Benito, G., Thorndycraft, V., & Rico, M. (2006). The topographic data source of digital terrain models as a key element in the accuracy of hydraulic flood modelling. Earth Surface Processes and Landforms, 31(4), 444–456. https://doi.org/10.1002/esp.1278

Directive - 2007/60/EC. *Directive 2007/60/EC of the European Parliament and of the Council of 23 October 2007 on the assessment and management of flood risks.* https://eur-lex.europa.eu/eli/dir/2007/60/oj

European Environmental Agency. (2021, January). Urban Atlas Land Cover/Land Use 2012 (Vector), Europe, 6-yearly. EEA Geospatial Data Catalogue. Retrieved February 6, 2025, from https://sdi.eea.europa.eu/catalogue/copernicus/api/records/debc1869-a4a2-4611-ae95-daeefce23490?language=all

Fowler, H. J., Lenderink, G., Prein, A. F., Westra, S., Allan, R. P., Ban, N., Barbero, R., Berg, P., Blenkinsop, S., X, H., DO, Guerreiro, S., Haerter, J. O., Kendon, E. J., Lewis, E., Schaer, C., Sharma, A., Villarini, G., Wasko, C., & Zhang, X. (2021). Anthropogenic intensification of short-duration rainfall extremes. Nature Reviews Earth & Environment, 2(2), 107–122. https://doi.org/10.1038/s43017-020-00128-6

Gichamo, T. Z., Sazib, N. S., Tarboton, D. G., & Dash, P. (2020). HydroDS: Data services in support of physically based, distributed hydrological models.

Environmental Modelling & Software, *125*, 104623. https://doi.org/10.1016/j.envsoft.2020.104623

Graceson, A., Hare, M., Monaghan, J., & Hall, N. (2013). The water retention capabilities of growing media for green roofs. Ecological Engineering, 61, 328–334. https://doi.org/10.1016/j.ecoleng.2013.09.030

Gröger, G., Kolbe, T. H., Nagel, C., & Häfele, K.-H. (2012). *OGC city geography markup language (CityGML) en- coding standard (OGC 12-019)*. Open Geospatial Consortium. Retrieved February 15, 2022, from http://www.opengis.net/spec/citygml/2.0

Hanssen-Bauer, I., Drange, H., Førland, E. J., Roald, L. A., Børsheim, K. Y., Hisdal, H., ... & Sorteberg, A. (2009). Climate in Norway 2100: Background information to NOU Climate Adaptation. *Klima i Norge*, *2100*.

Hemmati, M., Ellingwood, B. R., & Mahmoud, H. N. (2020). The role of urban growth in resilience of communities under flood risk. Earth S Future, 8(3). https://doi.org/10.1029/2019ef001382

Hernebring, C., Milotti, S., Kronborg, S. S., Wolf, T., & Mårtensson, E. (2015). Skyfallet i sydvästra Skåne 2014-08-31 fokuserat mot konsekvenser och relation till regnstatistik i Malmö. *Vatten*, *71*(2).

Huang, J., Kong, F., Yin, H., Middel, A., Liu, H., & Meadows, M. E. (2023). Green roof effects on urban building surface processes and energy budgets. Energy Conversion and Management, 287, 117100. https://doi.org/10.1016/j.enconman.2023.117100

Hutter, G. (2015). Collaborative governance and rare floods in urban regions – Dealing with uncertainty and surprise. Environmental Science & Policy, 55, 302–308. https://doi.org/10.1016/j.envsci.2015.07.028

Jha, A. K., Bloch, R., & Lamond, J. (2012). Cities and Flooding: A Guide to Integrated Urban Flood Risk Management for the 21st century. World Bank. https://openknowledge.worldbank.org/bitstream/10986/2241/1/667990PUB0Box30d0Flooding0Guidebook.pdf

Kabisch, N., & Haase, D. (2012). Green spaces of European cities revisited for 1990–2006. Landscape and Urban Planning, 110, 113–122. https://doi.org/10.1016/j.landurbplan.2012.10.017

Karteris, M., Theodoridou, I., Mallinis, G., Tsiros, E., & Karteris, A. (2016). Towards a green sustainable strategy for Mediterranean cities: Assessing the benefits of large-scale green roofs implementation in Thessaloniki, Northern Greece, using environmental modelling, GIS and very high spatial resolution remote sensing data. Renewable and Sustainable Energy Reviews, 58, 510–525. https://doi.org/10.1016/j.rser.2015.11.098

Kolbe, T., Kutzner, T., Smyth, C. S., Nagel, C., Roensdorf, C., & Heazel, C. (Eds.). (2021). OGC CITY GEOGRAPHY MARKUP LANGUAGE (CITYGML) PART 1: CONCEPTUAL MODEL STANDARD (OGC 20-010). Open Geospatial Consortium. Retrieved February 7, 2025, from http://www.opengis.net/doc/IS/CityGML-1/3.0

Köhler, M. (2006). Long-term vegetation research on two extensive green roofs in Berlin. Urban Habitats, 4(1), 3–26.

Länsstyrelserna. (2018). Recommendations for the handling of floods occuring as a result of extreme precipitation events – support for physical planning [*Rekommendationer för hantering av översvämning till följd av skyfall- stöd i fysisk planering*]. In https://www.lansstyrelsen.se (ISBN: 978 91 7281 818 7). Retrieved February 9, 2025, from https://www.lansstyrelsen.se/download/18.6efd95ae193bb06fa5815955/1734345334051/Rekommendationer%20f%C3%B6r%20hantering%20av%20%C3%B6versv%C3%A4mning%20till%20f%C3%B6ljd%20av%20skyfall%202018-5.pdf

Lehmann, J., Coumou, D., & Frieler, K. (2015). Increased record-breaking precipitation events under global warming. Climatic Change, 132(4), 501–515. https://doi.org/10.1007/s10584-015-1434-y

Nilsson, H., Pilesjö, P., Hasan, A., & Persson, A. (2022). Dynamic spatio-temporal flow modeling with raster DEMs. *Transactions in GIS*, *26*(3), 1572-1588. https://doi.org/10.1111/tgis.12870

Olsson, J., Berg, P., Eronn, A., Simonsson, L., Södling, J., Wern, L., Yang, W. (2017). Extremregn i nuvarande och framtida klimat – Analyser av observationer och framtidsscenarier. *SMHI Klimatologi*, Nr 47. https://www.smhi.se/publikationer-fran-smhi/sok-publikationer/2018-01-16-extremregn-i-nuvarande-och-framtida-klimat-analyser-av-observationer-och-framtidsscenarier

Pantazatou, K., Kanters, J., Olsson, P., Nyborg, J. L., & Harrie, L. (2023). Input data requirements for daylight simulations in urban densifications. Urban Informatics, 2(1). https://doi.org/10.1007/s44212-023-00024-6

Pantazatou, K., Mattisson, K., Olsson, P.-O., Telldén, E., Kettisen, A., Hosseinvash, S., Liu, W., & Harrie, L. (in press). Influence of land cover on noise simulation output – A case study in Malmö, Sweden. Noise Mapping. https://doi.org/10.1515/noise-2025-0016

Persson, A., Pilesjö, P., & Hasan, A. (2024). Dynamic modeling of urban hydrology in a geographic information system-setting with TFM-DYN. In Elsevier eBooks (pp. 315–336). https://doi.org/10.1016/b978-0-443-13605-4.00004-7

Pilesjö, P., & Hasan, A. (2014). A triangular form-based multiple flow algorithm to estimate overland flow distribution and accumulation on a digital elevation model. *Transactions in GIS*, *18*(1), 108-124. https://doi.org/10.1111/tgis.12015

Pizzileo, S., Moretti, G., & Orlandini, S. (2024). Flood plain inundation modeling with explicit description of land surface macrostructures. *Advances in Water Resources*, *188*, 104713, https://doi.org/10.1016/j.advwatres.2024.104713

Razzaghmanesh, M., Beecham, S., & Salemi, T. (2015). The role of green roofs in mitigating Urban Heat Island effects in the metropolitan area of Adelaide, South Australia. Urban Forestry & Urban Greening, 15, 89–102. https://doi.org/10.1016/j.ufug.2015.11.013

Robinson, A., Lehmann, J., Barriopedro, D., Rahmstorf, S., & Coumou, D. (2021). Increasing heat and rainfall extremes now far outside the historical climate. Npj Climate and Atmospheric Science, 4(1). https://doi.org/10.1038/s41612-021-00202-w

Schulte, C., & Coors, V. (Eds.). (2008). Development of a CityGML ADE for dynamic 3D flood information. Joint ISCRAM-CHINA and GI4DM Conference on Information Systems for Crisis Management, Harbin, China.

Shen, J., Zhou, J., Zhou, J., Herman, L., & Reznik, T. (2020). Constructing the CityGML ADE for the Multi-Source data integration of urban flooding. ISPRS International Journal of Geo-Information, 9(6), 359. https://doi.org/10.3390/ijgi9060359

Tuozzolo, S., Langhorst, T., De Moraes Frasson, R. P., Pavelsky, T., Durand, M., & Schobelock, J. J. (2019). The impact of reach averaging Manning's equation for an in-situ dataset of water surface elevation, width, and slope. Journal of Hydrology, 578, 123866. https://doi.org/10.1016/j.jhydrol.2019.06.038

Uggla, M., Olsson, P., Abdi, B., Axelsson, B., Calvert, M., Christensen, U., Gardevärn, D., Hirsch, G., Jeansson, E., Kadric, Z., Lord, J., Loreman, A., Persson, A., Setterby, O., Sjöberger, M., Stewart, P., Rudenå, A., Ahlström, A., Bauner, M., . . . Harrie, L. (2023). Future Swedish 3D City Models—Specifications, test data, and Evaluation. ISPRS International Journal of Geo-Information, 12(2), 47. https://doi.org/10.3390/ijgi12020047

UN (2018). 68% of the world population projected to live in urban areas by 2050, says UN | UN DESA | United Nations Department of Economic and Social Affairs. www.un.org. Retrieved February 5, 2025, from https://www.un.org/development/desa/en/news/population/2018-revision-of-world-urbanization-prospects.html

Williams, N. S. G., Lundholm, J., & MacIvor, J. S. (2014). FORUM: Do green roofs help urban biodiversity conservation? Journal of Applied Ecology, 51(6), 1643–1649. https://doi.org/10.1111/1365-2664.12333

Yan, W. Y., Shaker, A., & El-Ashmawy, N. (2014). Urban land cover classification using airborne LiDAR data: A review. Remote Sensing of Environment, 158, 295–310. https://doi.org/10.1016/j.rse.2014.11.001

Yang, H. S., Kang, J., & Choi, M. S. (2011). Acoustic effects of green roof systems on a low-profiled structure at street level. Building and Environment, 50, 44–55. https://doi.org/10.1016/j.buildenv.2011.10.004

APPENDIX

Table A.1 Numeric code representing every LC class included our study area.

NS-LC (Swedish)	NS-LC (English)	LC code	Infiltration (mm/h)
Anlagd och bebyggd mark; Andra anlagda ytor; Hårdgjord mark; Asfalt	Built-up surfaces; Other built-up surfaces; Hard ground; Asphalt	1	0
Anlagd och bebyggd mark; Andra anlagda ytor; Hårdgjord mark; Betong	Built-up surfaces; Other built-up surfaces; Hard ground; Concrete	2	0
Anlagd och bebyggd mark; Andra anlagda ytor; Hårdgjord mark; Gatsten	Built-up surfaces; Other built-up surfaces; Hard ground; Paving stone	3	1
Anlagd och bebyggd mark; Andra anlagda ytor; Hårdgjord mark; Gummibeläggning	Built-up surfaces; Other built-up surfaces; Hard ground; Rubber coating	4	0
Anlagd och bebyggd mark; Andra anlagda ytor; Hårdgjord mark; Konstgräs	Built-up surfaces; Other built-up surfaces; Hard ground; Artificial grass	5	2
Anlagd och bebyggd mark; Andra anlagda ytor; Hårdgjord mark; Kullersten	Built-up surfaces; Other built-up surfaces; Hard ground; Cobblestone	6	1
Anlagd och bebyggd mark; Andra anlagda ytor; Hårdgjord mark; Marksten	Built-up surfaces; Other built-up surfaces; Hard ground; Stone tiles	7	2
Anlagd och bebyggd mark; Andra anlagda ytor; Hårdgjord mark; Natursten	Built-up surfaces; Other built-up surfaces; Hard ground; Natural stone	8	0
Anlagd och bebyggd mark; Andra anlagda ytor; Hårdgjord mark; Packad grusbädd	Built-up surfaces; Other built-up surfaces; Hard ground; Gravel	9	20
Anlagd och bebyggd mark; Andra anlagda ytor; Schaktad mark; Schaktad mark	Built-up surfaces; Other built-up surfaces; Excavated ground; Excavated ground	10	30
Anlagd och bebyggd mark; Byggnadsytor; Byggnadsytor; Byggnadsytor	Built-up surfaces; Building surfaces; Building surfaces; Building surfaces	11	0
Anlagd och bebyggd mark; Väg- och järnvägsytor; Väg- och järnvägsytor; Väg- och järnvägsytor	Built-up surfaces; Road and railway surfaces; Road and railway surfaces; Road and railway surfaces	12	0
Öppen fastmark; Vegetationstäckt mark/låg vegetation; Buskmark	Open solid ground; Vegetated ground; Low vegetation; Shrubland	13	12
Öppen fastmark; Vegetationstäckt mark/låg vegetation; Gräsmark	Open solid ground; Vegetated ground; Low vegetation; Grassland	14	12
Vatten; Anlagt stilla vatten; Bassäng	Water; Manmade still water facilities; Pool	15	0
Vatten; Anlagt stilla vatten; Damm	Water; Manmade still water facilities; Dam	16	0
Anlagd och bebyggd mark; Byggnadsytor; Byggnadsytor; Byggnadsytor (grönt tak)	Built-up surfaces; Building surfaces; Building surfaces; Building surfaces (green roof)	17	12

The 1st column includes the full LC class name from the Swedish National Specifications for Land Cover (NS-LC), the 2nd column presents the English translation of the contents of column 1, and the 3rd column includes a corresponding numeric code. It should be noted that the contents of the 1st column correspond to a subset of the LC classes available in NS-LC that are found in our study area. The numbering in the numeric code representing every LC class in the table is arbitrary. The content of the last row (green roof) is not part of the NS-LC but was added strictly for the purposes of this study. The 4th column presents information on the infiltration capacity of the corresponding LC classes.

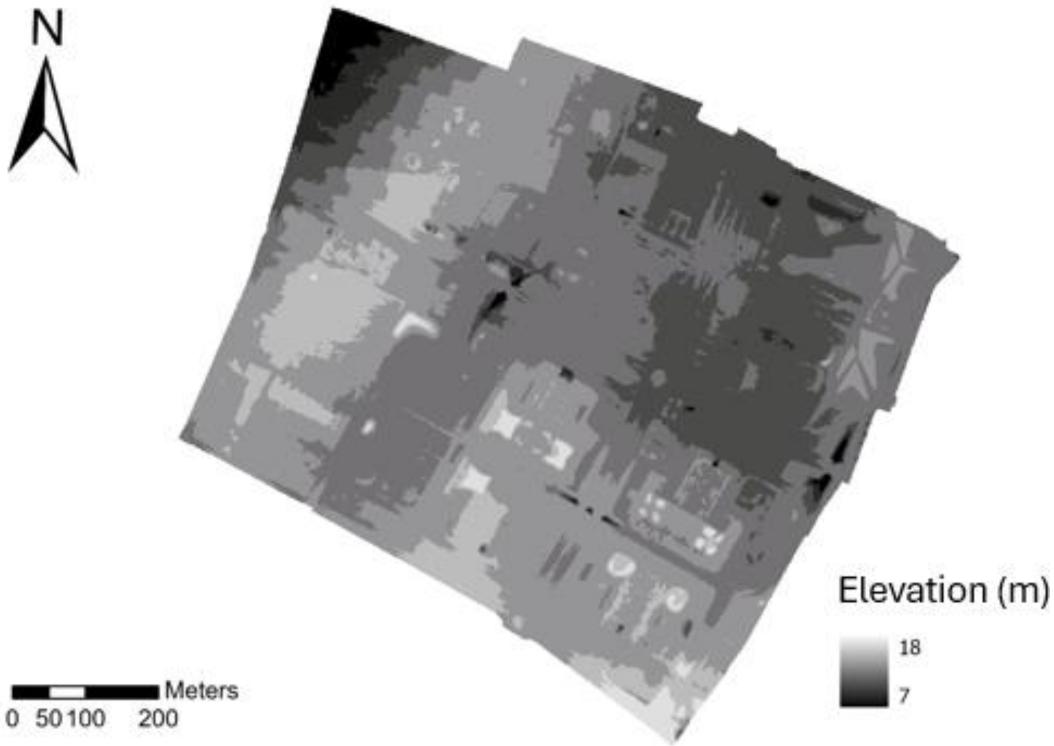

Figure A.1. Terrain elevation of the study area.

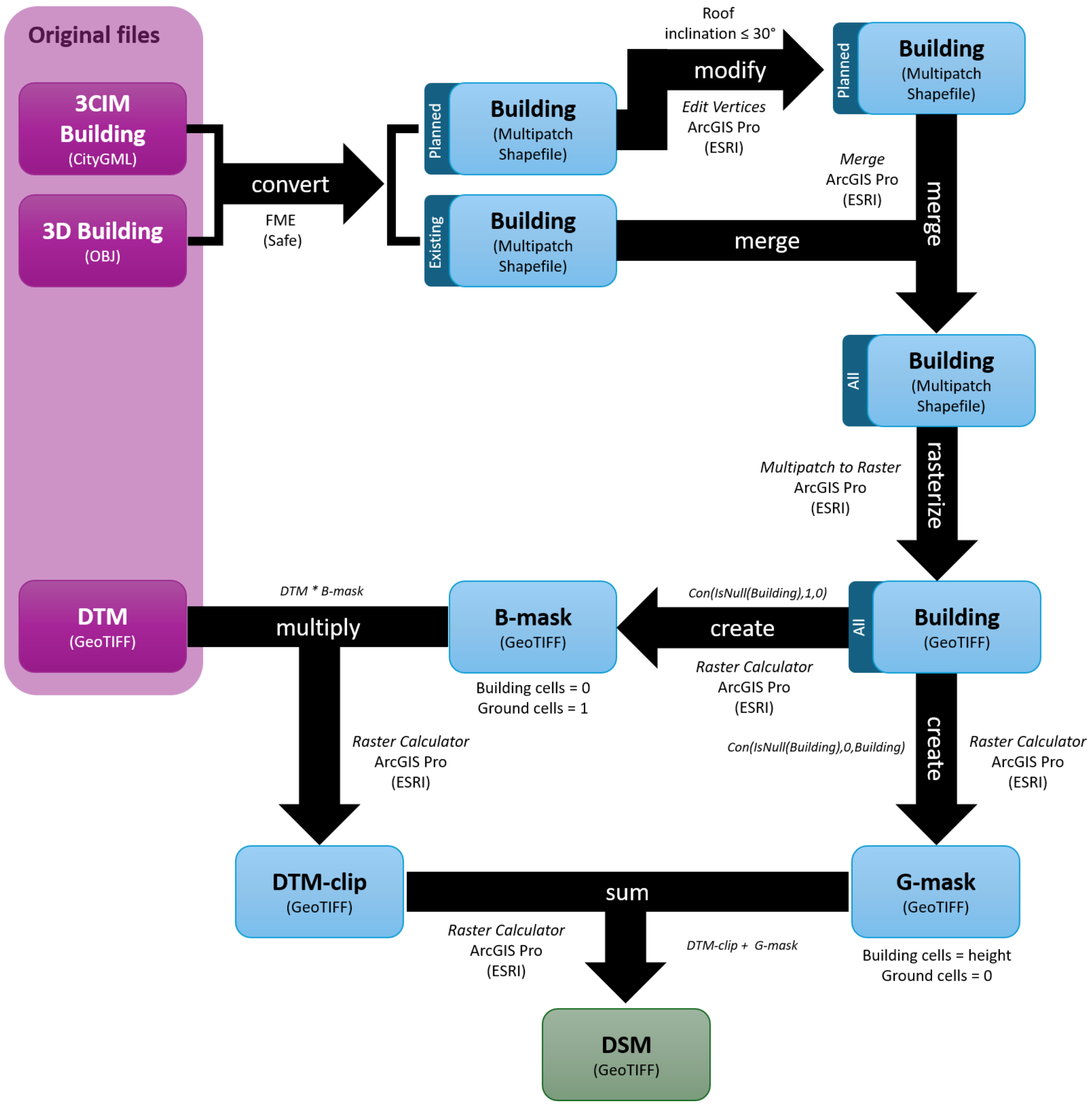

Figure A.2. Creation of DSM.

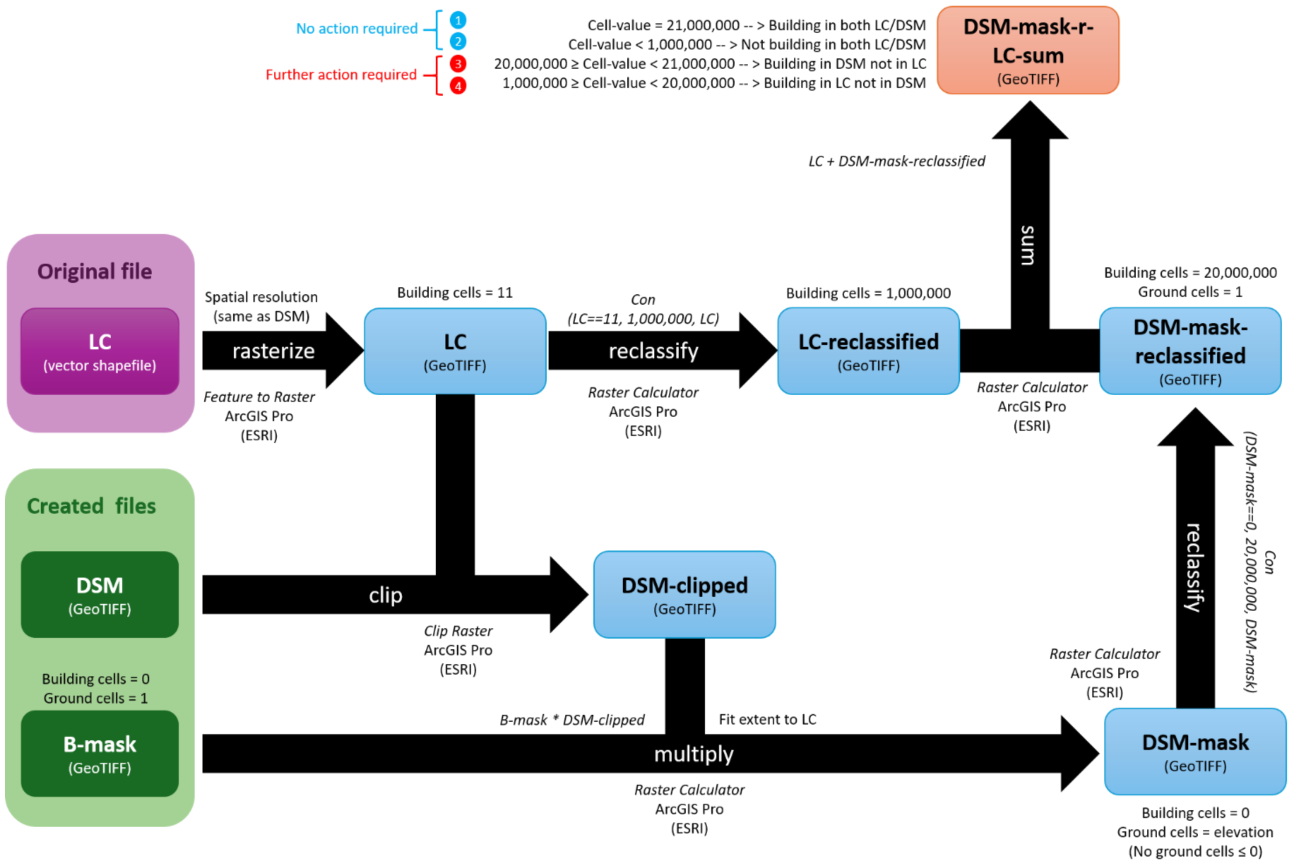

Figure A.3. Main process aligning DSM and LC datasets.

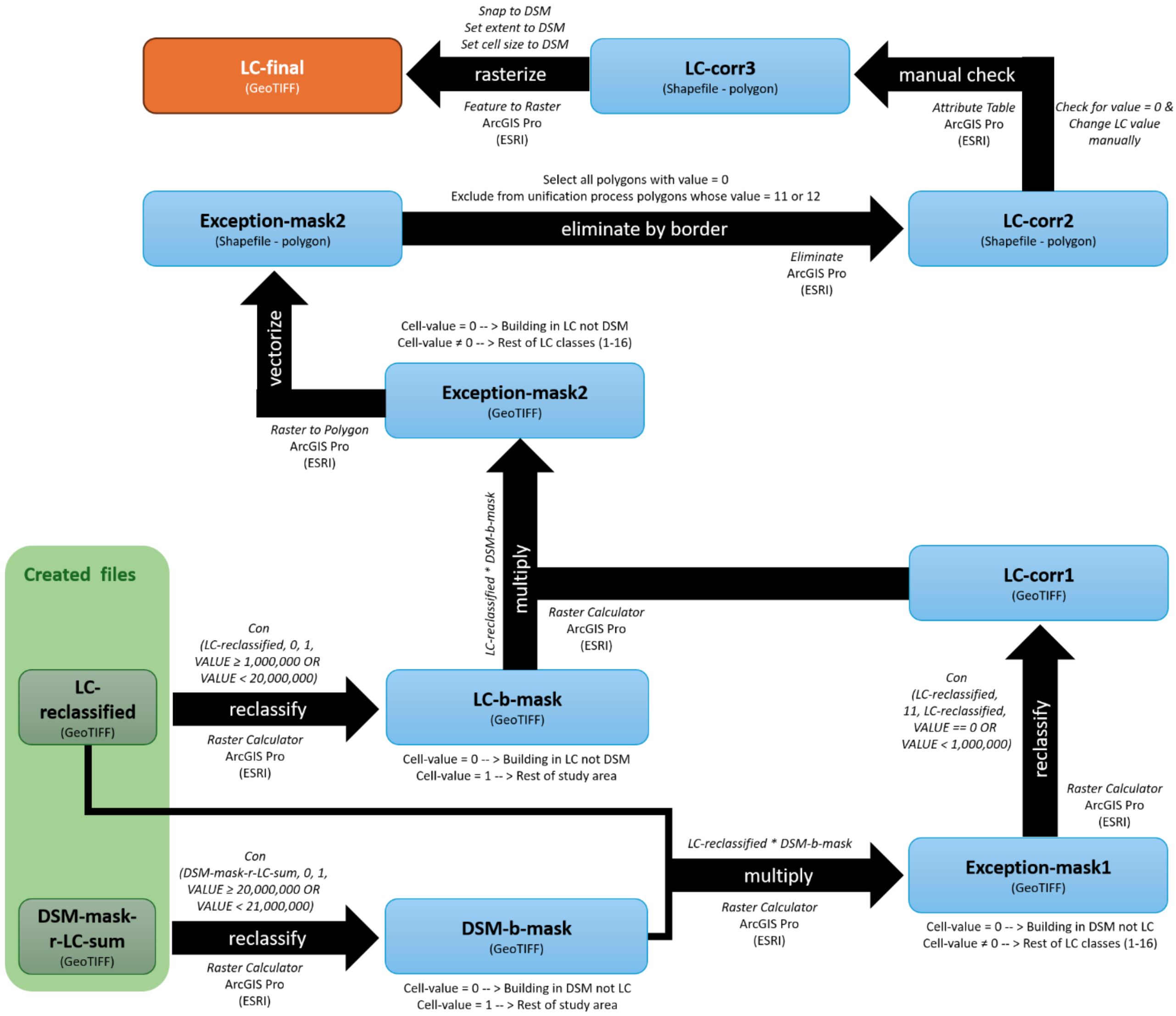

Figure A.4. Secondary process for aligning DSM and LC datasets (solution to problematic cases 3 & 4 from Figure A.3).